

Spectral Galerkin transfer operator methods in uniformly-expanding dynamics

Caroline Wormell

The University of Sydney

June 18, 2020

Introduction

- Interested in ergodic properties of chaotic systems: invariant measures, statistical limit laws, etc.
- Typically these quantities in general do not have explicit solutions: numerics are needed.
- Accurate, fast, transparent numerics that capitalise on smooth structure are important for extending understanding (c.f. PDEs, non-chaotic ODEs. . .)

Introduction

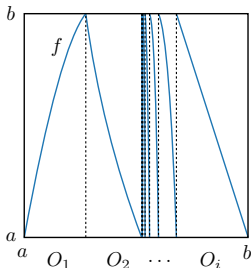
- Interested in ergodic properties of chaotic systems: invariant measures, statistical limit laws, etc.
- Typically these quantities in general do not have explicit solutions: numerics are needed.
- Accurate, fast, transparent numerics that capitalise on smooth structure are important for extending understanding (c.f. PDEs, non-chaotic ODEs. . .)

Goal: powerful numerics for smooth ergodic theory of a useful subclass of chaotic systems.

Chaotic maps

We consider maps of the interval $f : [a, b] \rightarrow [a, b]$ with nice properties:

- Countable partition $\overline{\bigcup_{i \in I} O_i} = [a, b]$,
 $f|_{O_i}$ bijections with inverses v_i
- Regularity conditions
on distortion $D_i := \log |v_i'|$, either:
 - $\sup_{s \leq r, i \in I} \|D_i^{(r)}\|_\infty \leq \infty$ for some r ;
 - D_i have unif. bounded analytic
extensions onto an open complex set
- Technical
requirement on placement of the O_i .
- Uniformly C-expanding. . .



Chaotic maps: Expansion condition

Standard condition is *uniformly expanding*:

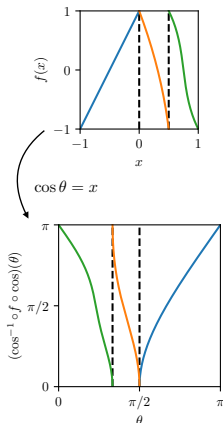
$$\inf_{x \in O_i, i \in I} |f'(x)| = \gamma > 1$$

We instead use *C-uniformly expanding*:

$$\inf_{x \in O_i, i \in I} \sqrt{\frac{1-x^2}{1-f(x)^2}} |f'(x)| = \tilde{\gamma} > 1,$$

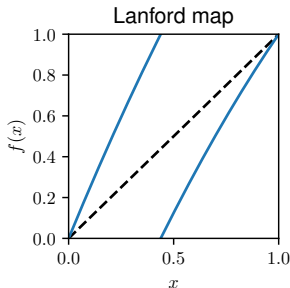
where domain $[a, b]$ is rescaled to $[-1, 1]$.

- $\iff \cos^{-1} \circ f \circ \cos$ unif. expanding
- If f is uniformly expanding then some f^n is C-unif. exp. (typically $n = 1$)



Examples of maps

- Tupling maps on $[0, 1]$, $f(x) = kx \pmod{1}$ for $k = 2, 3, \dots$
- Continued fraction maps, e.g. Gauss map on $[0, 1]$, $f(x) = x^{-1} \pmod{1}$, with change of variable $y = 2^x$
- Standard test map for numerics: Lanford map on $[0, 1]$, $f(x) = 2x + \frac{1}{2}x(1-x) \pmod{1}$ (see Figure)



Long-time statistical properties

These maps are chaotic with nice statistical properties. Two we are interested in:

- Absolutely continuous invariant measures (acims) ρ :

$$\frac{1}{N} \sum_{n=0}^{N-1} A(f^n(x_0)) \xrightarrow[\text{Leb.-a.e. } x_0]{N \rightarrow \infty} \int_a^b A \rho \, dx. \quad (*)$$

- Diffusion coefficients: CLT correction to (*) with variance

$$\sigma_f^2(A) = \sum_{n=-\infty}^{\infty} \int_a^b A \circ f^{|n|} \left(A - \int_a^b A \rho \, d\xi \right) dx,$$

well-defined if A is of bounded variation.

Transfer operator

The transfer operator $\mathcal{L} : \mathcal{B} \rightarrow \mathcal{B}$ tracks the action of the map f on signed measure densities in some Banach space \mathcal{B} of smooth functions:

$$\int_a^b A \circ f \varphi \, dx = \int_a^b A \mathcal{L}\varphi \, dx.$$

Has explicit formula for pointwise evaluation:

$$(\mathcal{L}\varphi)(x) = \sum_{i \in I} \sigma_i v_i'(x) \varphi(v_i(x)),$$

where v_i are the inverses of $f|_{O_i}$, and $\sigma_i = \text{sign } v_i'$.

Transfer operator

Statistical quantities of interest can be expressed in terms of linear algebraic properties of the transfer operator:

- Acim ρ satisfies

$$\begin{cases} \mathcal{L}\rho &= \rho, \\ \mathcal{S}\rho &= 1, \end{cases}$$

where $\mathcal{S}\varphi := \int_b^a \varphi dx$.

- Diffusion coefficient $\sigma_f^2(A)$ satisfies

$$\sigma_f^2(A) = \mathcal{S} \left[A \sum_{n=-\infty}^{\infty} \mathcal{L}^{|n|} (\rho A - \rho \mathcal{S}[\rho A]) \right]$$

In general, no explicit solutions!

Galerkin method

Take a family of finite-rank projections $\mathcal{P}_n : \mathcal{B} \rightarrow \mathcal{B}$ which asymptotically approximate the identity.

Pick large(ish) n :

- Compute the finite-dimensional operator $\mathcal{L}_n := \mathcal{P}_n \mathcal{L} \mathcal{P}_n|_{\text{im } \mathcal{P}_n}$.
- Substitute $\mathcal{P}_n \mathcal{L} \mathcal{P}_n|_{\text{im } \mathcal{P}_n}$ for \mathcal{L} in the problem of interest, e.g. for acim $\mathcal{P}_n \mathcal{L} \rho_n = \rho_n$.
- Numerically solve to get estimate: e.g. ρ_n should approximate true acim ρ .

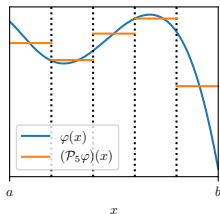
Galerkin method

Example: Ulam's method: $\mathcal{P}_n = L^2$ projection onto piecewise constant functions over even partition of size n .
If f is at least C^2 ,

$$\|\rho_n - \rho\|_{L^2} = \mathcal{O}(n^{-1} \log n).$$

Ulam is a very “low order” method:
basis functions have low regularity, with
consequent slow convergence of solutions
(in low regularity spaces).

In theory of differential equations, etc.
highest-order methods typically use a “spectral” basis of smooth
functions.

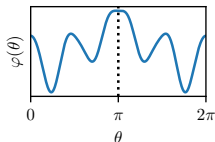


Spectral basis 1: Cosine series

Take an even C^1 function $\varphi : \mathbb{R}/2\pi\mathbb{Z} \rightarrow \mathbb{R}$.

We can write

$$\varphi(\theta) = \sum_{k=0}^{\infty} \hat{\varphi}_k \cos k\theta,$$



where

$$\hat{\varphi}_k = \frac{1}{\pi} \int_0^{\pi} \varphi(\theta) \cos k\theta \, d\theta.$$

Standard result that

$$|\hat{\varphi}_k| = O(s(k)) := \begin{cases} O(k^{-r}), & \varphi \in C^r \\ O(e^{-\delta k}), & \varphi \text{ bd. and analytic} \end{cases}$$

\mathbb{C}
on $\delta \overline{[0, 2\pi]}$.

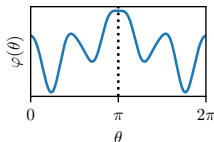
We call $s(\cdot)$ the “spectral” rate of convergence.

Spectral basis 1: Cosine series

Take an even C^1 function $\varphi : \mathbb{R}/2\pi\mathbb{Z} \rightarrow \mathbb{R}$.

We can write

$$\varphi(\theta) = \sum_{k=0}^{\infty} \hat{\varphi}_k \cos k\theta,$$



where

$$\hat{\varphi}_k = \frac{t_k}{\pi} \int_0^{\pi} \varphi(\theta) \cos k\theta \, d\theta.$$

Standard result that

$$|\hat{\varphi}_k| = \mathcal{O}(s(k)) := \begin{cases} \mathcal{O}(k^{-r}), & \varphi \in C^r \\ \mathcal{O}(e^{-\delta k}), & \varphi \text{ bd. and analytic} \end{cases}$$

\mathbb{C}
 on $\delta \overline{[0, 2\pi]}$.

We call $s(\cdot)$ the “spectral” rate of convergence.

Spectral basis 1: Cosine series

We can make the approximation

$$\varphi(\theta) = \sum_{k=0}^{K-1} \hat{\varphi}_k \cos k\theta + \mathcal{O}(K^{-s(K)}),$$

where

$$\hat{\varphi}_k = \frac{t_k}{\pi} \int_0^\pi \varphi(\theta) \cos k\theta \, d\theta.$$

Spectral basis 1: Cosine series

We can make the approximation

$$\varphi(\theta) = \sum_{k=0}^{K-1} \hat{\varphi}_k \cos k\theta + \mathcal{O}(Ks(K)),$$

where for $k = 0, \dots, K - 1$,

$$\hat{\varphi}_k = \frac{t_k}{K} \sum_{j=0}^{K-1} \varphi(\theta_{j,K}) \cos k\theta_{j,K} + \mathcal{O}(s(K)),$$

where $\theta_{j,K} := \frac{2j+1}{2K}\pi$.

Can compute all K Fourier coefficients with $\mathcal{O}(K \log K)$ operations using FFT algorithm.

Spectral basis 2: Chebyshev series

We can approximate a function

$\psi : [-1, 1] \rightarrow \mathbb{R}$ via cosine series theory

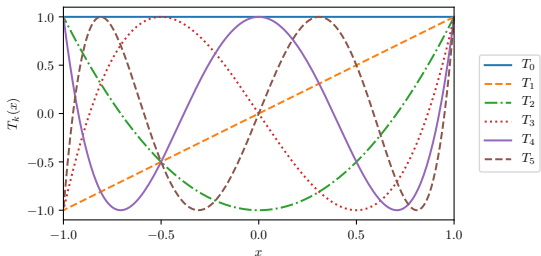
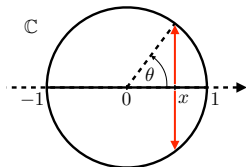
of $\varphi = \psi \circ \cos$.

The Chebyshev polynomials are, for

$x \in [-1, 1]$,

$$T_k(x) = \cos(k \cos^{-1} x).$$

They are orthogonal with respect to the weight $(1 - x^2)^{-1/2}$.



Spectral basis 2: Chebyshev series

Take a C^1 function $\psi : [-1, 1] \rightarrow \mathbb{R}$.

We can write

$$\psi(x) = \sum_{k=0}^{\infty} \check{\psi}_k T_k(x),$$

where

$$\check{\psi}_k = \frac{t_k}{\pi} \int_{-1}^1 \psi(x) T_k(x) \frac{dx}{\sqrt{1-x^2}}.$$

Have

$$|\check{\psi}_k| = \mathcal{O}(s(k)) := \begin{cases} \mathcal{O}(k^{-r}), & \psi \in C^r \\ \mathcal{O}(e^{-\delta k}), & \psi \text{ bd. and analytic on } \mathbb{C} \\ & e^\delta\text{-Bernstein ellipse } \overline{-1, 1}. \end{cases}$$

Spectral basis 2: Chebyshev series

Take a C^1 function $\psi : [-1, 1] \rightarrow \mathbb{R}$.

We can write

$$\psi(x) = \sum_{k=0}^{\infty} \check{\psi}_k T_k(x),$$

where

$$\check{\psi}_k = \frac{t_k}{\pi} \int_{-1}^1 \psi(x) T_k(x) \frac{dx}{\sqrt{1-x^2}},$$

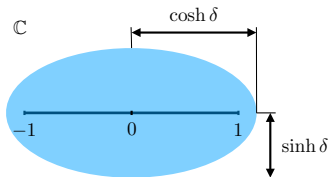
$t_k = 2 - \delta_{0k}$

Have

$$|\check{\psi}_k| = \mathcal{O}(s(k)) := \begin{cases} \mathcal{O}(k^{-r}), & \psi \in C^r \\ \mathcal{O}(e^{-\delta k}), & \psi \text{ bd. and analytic on } \mathbb{C} \\ & e^\delta\text{-Bernstein ellipse } \overline{-1, 1}. \end{cases}$$

Spectral basis 2: Chebyshev series

A Bernstein ellipse of parameter e^δ is $\cos \delta [0, 2\pi]$:



Spectral basis 2: Chebyshev series

We can make the approximation

$$\psi(x) = \sum_{k=0}^{K-1} \check{\psi}_k T_k(x) + \mathcal{O}(K^{-s(K)}),$$

where

$$\check{\psi}_k = \frac{t_k}{\pi} \int_{-1}^1 \psi(x) T_k(x) \frac{dx}{\sqrt{1-x^2}}.$$

Spectral basis 2: Chebyshev series

We can make the approximation

$$\psi(x) = \sum_{k=0}^{K-1} \check{\psi}_k T_k(x) + \mathcal{O}(K s(K)),$$

where

$$\check{\psi}_k = \frac{t_k}{K} \sum_{j=0}^{K-1} \psi(x_{j,K}) \cos kx_{j,K} + \mathcal{O}(s(K)),$$

where $x_{j,K} := \cos \theta_{j,K} = \cos \frac{2j+1}{2K} \pi$ are the Chebyshev points of the first kind.

Can compute all K Chebyshev coefficients with $\mathcal{O}(K \log K)$ operations using FFT algorithm.

Transfer operator discretisation

Choose projection \mathcal{P}_n to be projection onto first n Chebyshev coefficients, i.e.

$$\mathcal{P}_n \psi = \sum_{k=0}^{n-1} \check{\psi}_k T_k.$$

Then, if $\psi \in \text{im } \mathcal{P}_n$,

$$\mathcal{P}_n \mathcal{L} \psi = \sum_{j=0}^{n-1} \sum_{k=0}^{n-1} \mathcal{L}_{jk} \check{\psi}_k T_j$$

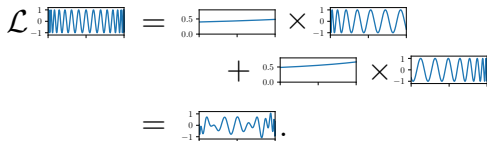
where \mathcal{L}_{jk} is the j th Chebyshev coefficient of $\mathcal{L} T_k$ (computable!).

Discretisation error

The transfer operator sends oscillating functions to functions of lower frequency:

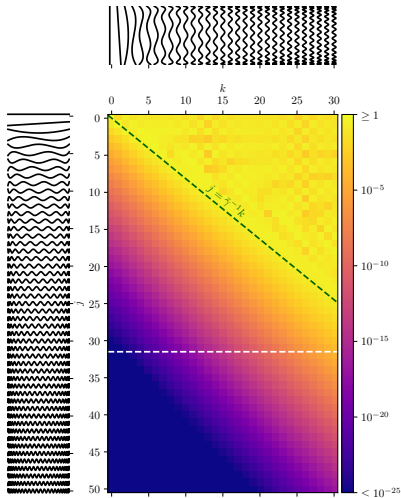
$$\mathcal{L}T_k = \sum_{i \in I} (\sigma_i v_i') \times (T_k \circ v_i).$$

Graphically,



Discretisation error

“Heat map” of $|\mathcal{L}_{jk}|$:



Convergence: bounds on $|\mathcal{L}_{jk}|$

$$\begin{aligned}
 \mathcal{L}_{jk} &= \frac{t_j}{\pi} \int_{-1}^1 (\mathcal{L}T_k)(x) T_j(x) \frac{dx}{\sqrt{1-x^2}} \\
 &= \frac{t_j}{2\pi} \int_0^{2\pi} (\mathcal{L}T_k)(\cos \theta) \cos j\theta \, d\theta \\
 &= \frac{t_j}{2\pi} \sum_{i \in I} \int_0^{2\pi} \underbrace{\sigma_i v_i'(\cos \theta)}_{h_i(\theta)} \cos k \underbrace{(\cos^{-1} v_i(\cos \theta))}_{w_i(\theta)} \cos j\theta \, d\theta \\
 &= \frac{t_j}{2\pi} \sum_{i \in I} \frac{1}{4} \sum_{\pm_1, \pm_2} \int_0^{2\pi} h_i(\theta) e^{i(\pm_1 k w_i(\theta) \pm_2 j\theta)} \, d\theta
 \end{aligned}$$

periodic integral
nice
oscillatory

Convergence: bounds on $|\mathcal{L}_{jk}|$

$$\begin{aligned}
 \mathcal{L}_{jk} &= \frac{t_j}{\pi} \int_{-1}^1 (\mathcal{L}T_k)(x) T_j(x) \frac{dx}{\sqrt{1-x^2}} \\
 &= \frac{t_j}{2\pi} \int_0^{2\pi} (\mathcal{L}T_k)(\cos\theta) \cos j\theta \, d\theta \\
 &= \frac{t_j}{2\pi} \sum_{i \in I} \int_0^{2\pi} \underbrace{\sigma_i v_i'(\cos\theta)}_{h_i(\theta)} \cos k \underbrace{(\cos^{-1} v_i(\cos\theta))}_{w_i(\theta)} \cos j\theta \, d\theta \\
 &= \frac{t_j}{2\pi} \sum_{i \in I} \frac{1}{4} \sum_{\pm_1, \pm_2} \int_0^{2\pi} h_i(\theta) e^{i(\pm_1 k w_i(\theta) \pm 2j\theta)} \, d\theta
 \end{aligned}$$

periodic integral
nice
oscillatory

h_i can be general: could treat weights other than v_i' .

Convergence: bounds on $|\mathcal{L}_{jk}|$

Let's suppose that v_i is analytic on a δ -Bernstein ellipse. Then h_i, w_i are analytic on a complex strip of half-width δ .

We can move the contour of integration by $i\delta$:

$$\begin{aligned} & \int_0^{2\pi} h_i(\theta) e^{i(kw_i(\theta) - j\theta)} d\theta \\ &= \int_0^{2\pi} h_i(\theta + i\delta) e^{ikw_i(\theta + i\delta) - ij(\theta + i\delta)} d\theta \\ &= \int_0^{2\pi} h_i(\theta + i\delta) e^{i(w_i(\theta)k - j\delta) - \delta(j - w_i'(\theta)k) + k\mathcal{O}(\delta^2)} d\theta \end{aligned}$$

So

$$\left| \int_0^{2\pi} h_i(\theta) e^{i(kw_i(\theta) - j\theta)} d\theta \right| \leq \|h_i(\cdot + i\delta)\|_1 e^{-\delta(j - \gamma^{-1}k) + \mathcal{O}(k\delta^2)}$$

Convergence: bounds on $|\mathcal{L}_{jk}|$

Theorem (W. '19)

For all $p > \check{\gamma}^{-1}$ there exists C such that

$$|\mathcal{L}_{jk}| \leq C \min\{1, s(j - pk)\},$$

where s is the spectral convergence rate.

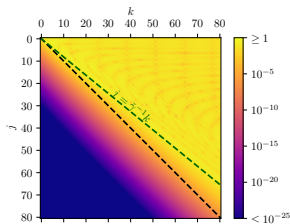


Figure: Heat map of $|\mathcal{L}_{jk}|$ for the Lanford map

Solution operator

We will find estimates for acim, diffusion coefficient, etc. using *solution operator*:

$$\mathcal{S} = (\text{id} - \mathcal{L} + 1.\mathcal{S})^{-1}$$

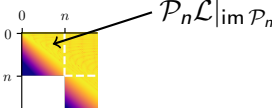
resolvent of \mathcal{L} rank 1 perturbation with left eig'f'n \mathcal{S}

Has useful properties:

- $\mathcal{S}1 = \rho$
- $\mathcal{S}\varphi = \sum_{k=0}^{\infty} \mathcal{L}^k \varphi$ if $\int_{-1}^1 \varphi dx = 0$
 - Hence $\sigma_f^2(A) = \mathcal{S} [A(2\mathcal{S} - \text{id})(\rho A - \rho \mathcal{S}[\rho A])]$

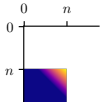
Convergence of estimates: operator error

The solution operator is a simple matrix function of \mathcal{L} . We use near-upper-triangularity of \mathcal{L} in Chebyshev basis, computing with:

$$\tilde{\mathcal{L}}_n := \mathcal{L} - (\text{id} - \mathcal{P}_n)\mathcal{L}\mathcal{P}_n =$$


The diagram shows a square matrix with a vertical axis and a horizontal axis, both labeled with 0 and n. A dashed vertical line is drawn at index n. The region above this line and to the left of the diagonal is shaded yellow, representing the upper triangular part of the matrix. The region below the dashed line and to the left of the diagonal is shaded purple, representing the lower triangular part. An arrow points from the label $\mathcal{P}_n \mathcal{L} |_{\text{im } \mathcal{P}_n}$ to the yellow region.

For Banach space \mathcal{B} (e.g. BV) and $\epsilon < 1$ depending on \mathcal{B} , standard relationships between norms and Chebyshev coefficients give

$$\|\tilde{\mathcal{L}}_n - \mathcal{L}\|_{\mathcal{B}} = \left\| \begin{array}{c} 0 \quad n \\ 0 \quad \text{---} \\ n \end{array} \right\|_{\mathcal{B}} = \mathcal{O}(n^{1+\epsilon} s(n)).$$


The diagram shows a square matrix with a vertical axis and a horizontal axis, both labeled with 0 and n. A dashed vertical line is drawn at index n. The region below this line and to the left of the diagonal is shaded purple, representing the lower triangular part of the matrix difference.

Convergence of estimates: operator error

Then, since \mathcal{S} is just an operator function of $1\mathcal{S}$ (which is upper-triangular) and \mathcal{L} , if

$$\tilde{\mathcal{S}}_n := (\text{id} - \tilde{\mathcal{L}}_n + 1\mathcal{S})^{-1}$$

then

$$\|\tilde{\mathcal{S}}_n - \mathcal{S}\|_{\mathcal{B}} = \mathcal{O}(n^{1+\epsilon} s(n)),$$

and by block-upper-triangularity we can compute

$$\tilde{\mathcal{S}}_n|_{\text{im } \mathcal{P}_n} = (\text{id} - \mathcal{L}_n + 1\mathcal{S}|_{\text{im } \mathcal{P}_n})^{-1}.$$

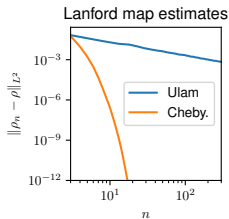
(NB: also possible to use bounds on $|\mathcal{L}_{jk}|$ for estimates in the style of Keller and Liverani '99.)

Computational complexity

Complexity of spectral Galerkin method:

- $n \times \mathcal{O}(n \log n)$ for computation of $\mathcal{P}_n \mathcal{L}|_{\text{im } \mathcal{P}_n}$, plus
- $\mathcal{O}(n^3)$ for matrix inversion to get solution operator is

$\mathcal{O}(n^3)$ complexity overall, vs $\mathcal{O}(n^{1+\epsilon} s(n))$ decay in error.

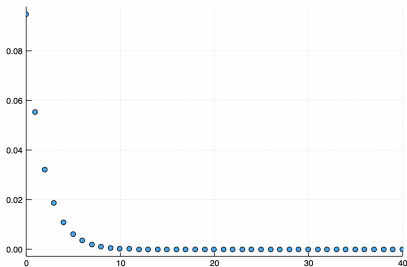


Method	Error	Complexity	Error vs Cxty C
Ulam	$\mathcal{O}(n^{-1} \log n)$	$\mathcal{O}(n)$	$\mathcal{O}(C^{-1} \log C)$
Dynamical zeta	$\mathcal{O}(e^{-kn^2})$	$ I ^n$	$\mathcal{O}(e^{-k'(\log_{ I } C)^2})$
Chebyshev	$\mathcal{O}(e^{-\delta n})$	$\mathcal{O}(n^3)$	$\mathcal{O}(e^{-\delta' C^{1/3}})$

Table: Comparison of error vs complexity for an analytic map

Poltergeist.jl

```
[julia> lyapunov(L) ]  
0.6576617800065931  
  
[julia> birkhoffvar(L,A) # diffusion coefficient ]  
0.36010948619915506  
  
[julia> scatter(0:40,covariancefunction(L,A,40),xlim=(0,40),legend=false) ]
```



More examples: <https://github.com/wormell/Poltergeist.jl>

Validated bounds

A dramatic example of validated bounds (Theorem 2.5, W. '19):

- a** The Lanford map's Lyapunov exponent $L_{exp} := \int_{\Lambda} \log |f'| \rho dx$ lies in the range

$$L_{exp} = 0.657\ 661\ 780\ 006\ 597\ 677\ 541\ 582\ 413\ 823\ 832\ 065\ 743\ 241\ 069\ 580\ 012\ 201\ 953\ 952\ 802\ 691\ 632\ 666\ 111\ 554\ 023\ 759\ 556\ 459\ 752\ 915\ 174\ 829\ 642\ 156\ 331\ 798\ 026\ 301\ 488\ 594\ 89 \pm 2 \times 10^{-128}.$$

- b** The diffusion coefficient for the Lanford map with observable $A(x) = x^2$ lies in the range

$$\sigma_f^2(A) = 0.360\ 109\ 486\ 199\ 160\ 672\ 898\ 824\ 186\ 828\ 576\ 749\ 241\ 669\ 997\ 797\ 228\ 864\ 358\ 977\ 865\ 838\ 174\ 403\ 103\ 617\ 477\ 981\ 402\ 783\ 211\ 083\ 646\ 769\ 039\ 410\ 848\ 031\ 999\ 960\ 664\ 7 \pm 6 \times 10^{-124}.$$

These results were obtained in 9 hours on a research server (mostly computing \mathcal{S} , which is reusable).

Related results

- Slipantschuk and Bandtlow ('20): using Chebyshev approximation of analytic expanding maps, eigendata converges exponentially.
- Crimmins and Froyland ('19): statistical properties that are functions of the transfer operator (e.g. large deviations) can be estimated using transfer operator discretisations.

Application: Pomeau-Manneville systems

Interested in statistical properties of *non*-uniformly expanding maps

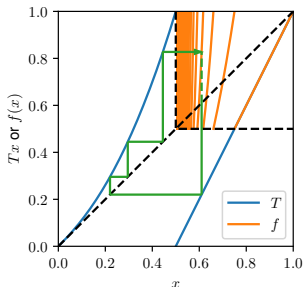
$$T : [0, 1] \circlearrowright$$

$$T_x = \begin{cases} x(1 + 2^\alpha x^\alpha), & x \leq \frac{1}{2}, \\ 2x - 1, & x > \frac{1}{2}, \end{cases}$$

where $\alpha > 0$.

For example, absolutely continuous invariant measures: for $\alpha \geq 1$ this is infinite ergodic theory.

- Lack of uniform expansion and weak mixing properties makes numerics very challenging.
- Ulam-style methods very slow, non-viable for α much greater than 1.



Application: Pomeau-Manneville systems

We approach via induced map

$$f : [\frac{1}{2}, 1] \circlearrowleft:$$

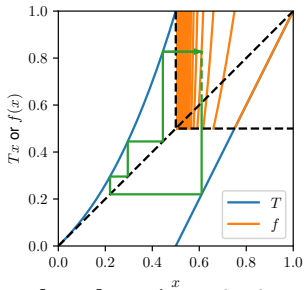
$$f(x) := T^{\tau_T(x)} x.$$

This map is analytic and full-branch uniformly-expanding: we can use Chebyshev methods on it.

Theorem (W., forthcoming)

There exists a real-analytic function $A : (0, 1] \rightarrow [0, \infty)^x$ such that

$$f(x) = A^{-1}(A(x) \bmod 1),$$



Application: Pomeau-Manneville systems

The transfer operator of f is

$$(\mathcal{L}_f \varphi)(x) = \sum_{n=0}^{\infty} \frac{A'(x)}{2} \frac{\varphi(A^{-1}(A(2x-1) + n))}{A'(A^{-1}(A(2x-1) + n))}.$$

Problem: the terms in the sum decay very slowly!

Solution: use smoothness. When $\varphi = T_k$ (i.e. smooth), can use Euler-Maclaurin formula to accurately evaluate $(\mathcal{L}_f \varphi)(x)$.

Application: Pomeau-Manneville systems

Effective estimates of statistical properties of both the induced map and the full, non-uniformly expanding map, for a wide range of α :

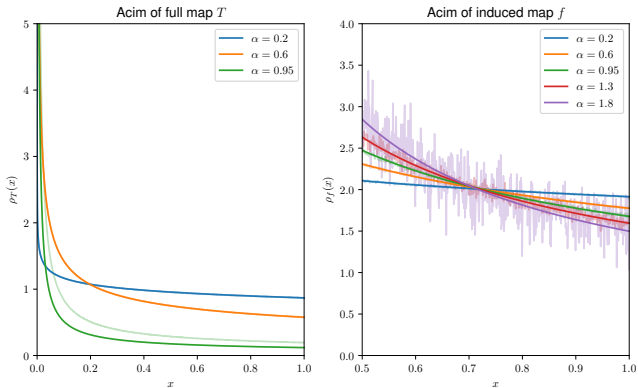


Figure: Acims of the full map with different normalisations. Pale colours indicate estimates from binning on 10^8 simulations.

Application: Pomeau-Manneville systems

Very accurate validated bounds again possible.

For example, the expected return time to $[1/2, 1]$ for $\alpha = 0.95$ (a near-singular case) lies in the range

$$\mathbb{E}_f[\tau_T] = 14.073\ 323\ 220\ 001\ 939\ 529\ 241\ 549\ 699\ 610\ 756\ 609\ 803\ 3171 \pm 10^{-43}.$$

Application: Chaotic hypothesis

Joint work with Georg Gottwald

Chaotic hypothesis (Gallavotti-Cohen)

The macroscopic dynamics of a (high-dimensional) chaotic system on its attractor can be regarded as a transitive hyperbolic (“Anosov”) evolution.

- We derive a “thermodynamic” limiting system of a large self-coupled ensemble of uniformly-expanding maps.
- We use Poltergeist to discover non-hyperbolic dynamics in the limiting system.

Application: Chaotic hypothesis

Consider an ensemble of $M \gg 1$ microscopic constituents $q^{(j)} \in [-1, 1]$ with uniformly expanding dynamics:

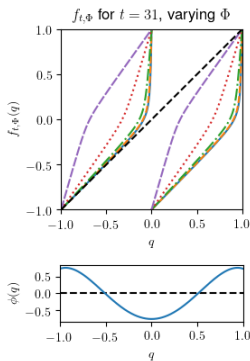
$$q_{n+1}^{(j)} = f_{t, \Phi_n}(q_n^{(j)}), \quad j = 1, \dots, M.$$

The mean-field

$$\Phi_n = \frac{1}{M} \sum_{j=0}^{\infty} \phi(q_n^{(j)})$$

feeds back into the $q^{(j)}$.

External parameter t which regulates the strength of the feedback.



Application: Chaotic hypothesis

Let $\mu_n(q) dq$ be the empirical measure of the $q_n^{(j)}$. Then:

- Dynamics can be formulated

$$\mu_{n+1} = F_t(\mu_n) := \mathcal{L}_{t;\int \phi \mu_n dq} \mu_n$$

where $\mathcal{L}_{t;\phi}$ is the transfer operator of $f_{t;\phi}$.

- Mean-field observables (i.e. “macroscopic” dynamics) are expectations over $\mu_n(q) dq$;
- In “thermodynamic” limit $M \rightarrow \infty$ reasonable to take $\mu_0 \in C^1$
 \implies can study dynamics with Chebyshev methods.

Application: Chaotic hypothesis

The following Poltergeist function iterates μ_n :

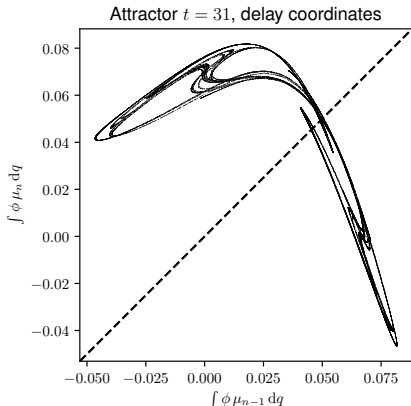
```
function F(mu, t)
    Phi = sum(phi * mu) # 'sum' = total integral
    f = fmap(t,Phi) # predefined initialiser
    return transfer(f,mu)
end
```

For standard double-floating-point implementation this routine evaluates in around 1 millisecond, accurate in norm to $\approx 10^{-13}$.

More details at tinyurl.com/pg-selfcoupled.

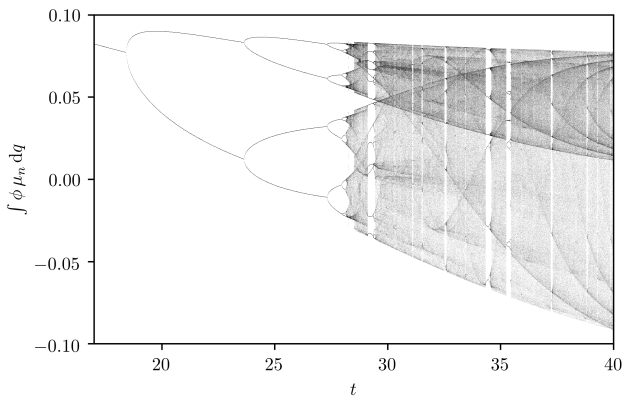
Application: Chaotic hypothesis

- For large t , macroscopic dynamics are chaotic, with quasi-unimodal dynamics in $\Phi_n = \int \phi \mu_n dq$.



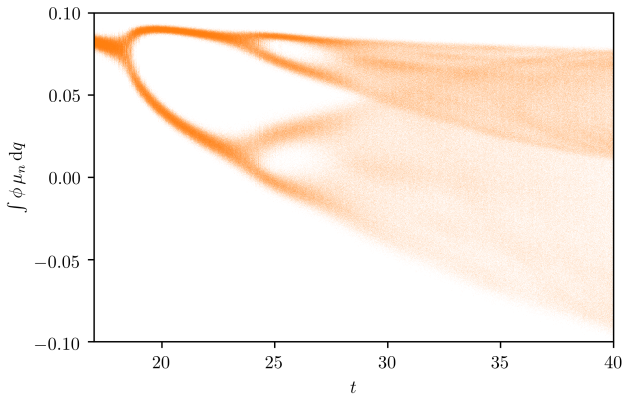
Application: Chaotic hypothesis

Clearly see Henon/logistic-like orbit plot—indicating non-hyperbolicity (W. and Gottwald, '19)



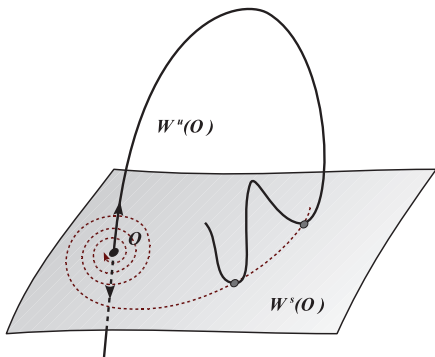
Application: Chaotic hypothesis

Compare with simulations using large, finite $M = 300,000$:



Application: Chaotic hypothesis

Using Poltergeist, we have found direct evidence of non-hyperbolicity in the limit system: a homoclinic tangency.



(Gonchenko *et al*, '12)

Application: Chaotic hypothesis

For $30 \leq t \leq 31$ there is a fixed point $\mu_t^* = F_t(\mu_t^*)$ with $\int \phi \mu_t^* dq \approx 0.05$.

At this fixed point, the Jacobian $J_{\mu_t^*} F_t$ has a single unstable eigenvalue $\lambda_t \sim -1.6$ with (normalised) eigenfunction v_t .

The unstable manifold W_t^u is locally parametrised

$$W_t^u(a) = \mu_t^* + v_t a + \frac{1}{2} h_t a^2 + \mathcal{O}(a^3),$$

with

$$W_t^u(\lambda_t a) = F_t(W_t^u(a)).$$

(Thus, $\{W_t^u(\lambda_t^m a) : m \in \mathbb{Z}\}$ is an orbit originating from μ_t^* .)

Application: Chaotic hypothesis

For a homoclinic, we need the orbit to return to μ_t^* :

$$\lim_{m \rightarrow \infty} W_t^u(\lambda_t^m a) - \mu_t^* = 0 \quad (1)$$

Along the stable manifold, the unstable vector at $W_t^u(a)$ is given by

$$v_{t,a} \propto \frac{d}{da} W_t^u(a) = v_t + h_t a + \mathcal{O}(a^2).$$

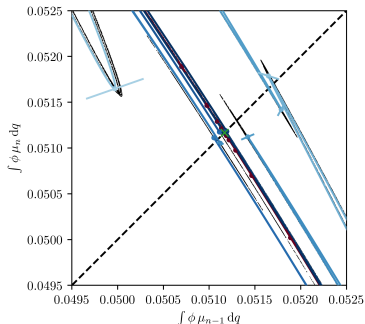
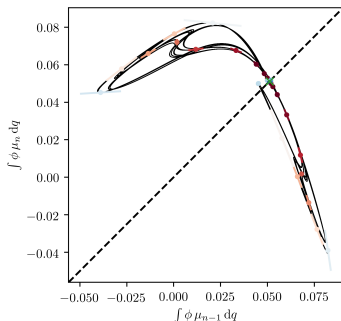
For a stable-unstable tangency $v_{t,a}$ must also be a stable vector, i.e.

$$\lim_{m \rightarrow \infty} J_{F_t^m} W_t^u(a)[v_{t,a}] = 0. \quad (2)$$

Thus, a homoclinic tangency can be found by searching for (a, t) such that (1-2) both hold. We can do this quite efficiently with Poltergeist (as yet no theorems).

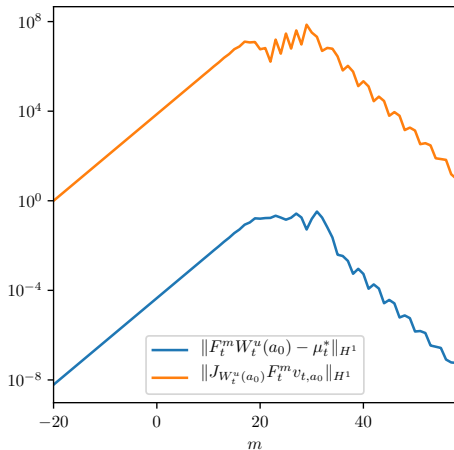
Application: Chaotic hypothesis

Using Poltergeist the following homoclinic tangency was found at $t = 30.0618314$:



Application: Chaotic hypothesis

Error probably of order $\sim 10^{-8}$:



Conclusion

Chebyshev Galerkin transfer operator methods for chaotic systems:

- Harness smooth structure of the problem
- Are very efficient and very accurate
- Can be harnessed profitably for study of more complex phenomena in chaotic dynamics.